



**HAL**  
open science

## **Data communication using blue GaN-on-Si micro-LEDs reported on a 200-mm Silicon substrate**

Sultan El Badaoui, Luc Maret, Nicolas Delaunay, Anthony Cibié, Patrick Le Maitre, Clement Ballot, Julia Simon, Bastien Miralles, Bernard Aventurier, Paolo De Martino, et al.

### ► To cite this version:

Sultan El Badaoui, Luc Maret, Nicolas Delaunay, Anthony Cibié, Patrick Le Maitre, et al.. Data communication using blue GaN-on-Si micro-LEDs reported on a 200-mm Silicon substrate. *IEEE Photonics Technology Letters*, 2024, 36 (18), pp.1149-1152. <10.1109/LPT.2024.3451244>. <hal-04681830>

**HAL Id: hal-04681830**

**<https://hal.univ-grenoble-alpes.fr/hal-04681830v1>**

Submitted on 27 Jan 2025

**HAL** is a multi-disciplinary open access archive for the deposit and dissemination of scientific research documents, whether they are published or not. The documents may come from teaching and research institutions in France or abroad, or from public or private research centers.

L'archive ouverte pluridisciplinaire **HAL**, est destinée au dépôt et à la diffusion de documents scientifiques de niveau recherche, publiés ou non, émanant des établissements d'enseignement et de recherche français ou étrangers, des laboratoires publics ou privés.



HAL Authorization

# Data communication using blue GaN-on-Si micro-LEDs reported on a 200-mm Silicon substrate

Sultan El Badaoui, Luc Maret, Nicolas Delaunay, Anthony Cibié, Patrick Le Maitre, Clement Ballot, Julia Simon, Bastien Miralles, Bernard Aventurier, Paolo De Martino, Stephanie Jacob and Yannis Le Guennec

**Abstract**—In this paper, Gallium Nitride (GaN) blue micro-Light-Emitting-Diodes ( $\mu$ LEDs) reported on a 200-mm Silicon substrate are utilized for multi-Gb/s data transmission. The manufacturing process is compatible with CMOS integrated circuit design, paving the way for fully integrated transmitters for  $\mu$ LED-based visible light communications (VLC) or chip-to-chip interconnects. Fiber-guided transmission has been realized using direct current optical-orthogonal frequency division multiplexing (DCO-OFDM) modulation, and a data rate of 5.9 Gb/s at a Bit-Error-Rate (BER) of  $3.8 \times 10^{-3}$  is reported using a single  $50 \times 50 \mu\text{m}^2$  blue  $\mu$ LED. This data rate was further improved to reach 15.5 Gb/s in the case where the  $\mu$ LED is only limited by its non-linear distortions instead of the system's noise, highlighting the high linearity of GaN  $\mu$ LEDs.

**Index Terms**— Chip-to-chip communication, DCO-OFDM, GaN micro-LED, Optical communication.

## I. INTRODUCTION

IN parallel to their continuous development in the field of micro-display [1], GaN  $\mu$ LEDs have emerged as a strong candidate for data transmission for Visible Light Communication (VLC) [2][3][4] and chip-to-chip interconnects [5]. (In)GaN LEDs can emit in the blue and green visible range by adjusting the Indium concentration in the emitting region. Initially designed for lighting applications thanks to their high efficiency in the blue range, these LEDs have continuously evolved throughout the years in terms of size and efficiency. Eventually, it became possible to reduce their size to the micrometer scale while mitigating their loss of efficiency, paving the way for high-resolution micro-displays necessary for virtual reality (VR) and augmented reality (AR) development. In addition to their high brightness, the GHz-range modulation bandwidth makes GaN  $\mu$ LEDs attractive for VLC applications as well, where bandwidths of more than 1 GHz have been demonstrated [6][7], and data rates from a few hundred Mb/s [8] to several Gb/s [9][10] have been reported, using spectrally efficient optical orthogonal frequency division multiplexing (O-OFDM). Although most work on VLC has focused on wireless applications, the continuous reduction in  $\mu$ LED pitch, increase in modulation bandwidth and efficiency

is opening the possibility for guided light applications, mainly short-range ( $< 10\text{m}$ ) chip-to-chip communication as a solution for the interconnect bottleneck problem [5]. Indeed, the ability of high-density integration of GaN  $\mu$ LEDs, thanks to their low pitch (down to a few micrometers), allows for a high-density parallel communication scheme utilizing multi-core optical fibers. Continuous developments directed at reducing their pitch size for higher data density while improving efficiency and bandwidth, aim to have GaN interconnects that can achieve  $> 1 \text{ Tb/s/mm}^2$  at a link energy consumption of  $< 1 \text{ pJ/bit}$ . Achieving such numbers can situate GaN interconnects as a serious contender in the short-range interconnect field, in comparison to silicon photonics for example which require bulky laser sources. It is important to note that, generally, the motivation behind using visible light for communication arises from the inherent benefits of using this part of the spectrum, since it is unlicensed, provides short range secured transmissions and does not interfere with the radiofrequency (RF) spectrum. However, in our case, the main motivation is about using GaN  $\mu$ LEDs because of their distinctive properties such as high luminosity, manufacturability and resilience to high temperatures.

In 2020, a data rate of 7.7 Gb/s was demonstrated using a single blue  $10 \times 10 \mu\text{m}^2$  (In)GaN  $\mu$ LED operated at  $25.5 \text{ kA/cm}^2$  and DCO-OFDM [4]. After this demonstration, a data rate of 7.91 Gb/s was reached using a single  $435 \mu\text{m}^2$  violet  $\mu$ LED, further improved to 11.95 Gb/s when considering only the  $\mu$ LED non-linear distortions [11]. However,  $\mu$ LEDs used in the aforementioned results were grown on Sapphire substrates that are currently not compatible with 200-mm and future 300-mm integration of application-specific integrated circuits (ASICs) integrating OFDM modulators,  $\mu$ LED drivers and digital-to-analog converters. For joint ASIC and  $\mu$ LED integration, a fabrication process based on Silicon (Si) substrates is highly desirable. Nevertheless, it is known that GaN  $\mu$ LEDs grown on Silicon wafers (GaN-on-Si  $\mu$ LEDs) exhibit a higher defect density compared to those grown on free-standing GaN or Sapphire, which is primarily attributed to the large lattice mismatch between GaN and Si (17%) and the significant 56% difference in the thermal expansion coefficient between Si and

This work is part of the IPCEI Microelectronics and Connectivity project and was supported by the French Public Authorities within the frame of France 2030.

All the authors in this paper except Y. Le Guennec are affiliated to Université Grenoble Alpes, CEA-LETI, 17 Rue Des Martyrs, 38054 Grenoble, France

(email: sultan.elbadaoui@cea.fr)

Authors Y. Le Guennec and S. El Badaoui are part of Université Grenoble Alpes, CNRS, Grenoble INP, GIPSA-lab, 38000 Grenoble, France (email: yannis.le-guennec@grenoble-inp.fr)

Ga [12].

In this work, we present data transmission results using a single  $50 \times 50 \mu\text{m}^2$  GaN-on-Si blue  $\mu\text{LED}$ , which is, to our knowledge, the first time a communication demonstration is performed on GaN  $\mu\text{LED}$ s fabricated through a 200-mm process compatible with monolithic ASIC integration.

The paper is organized as follows: Section II describes the LED design, Section III demonstrates the characteristics of the  $\mu\text{LED}$ s through DC and RF characterizations, Section IV introduces the experimental setup and data rate measurements, and Section V concludes with the results.

## II. DEVICE

The wafer used is from a commercial 200-mm GaN-on-Si(111) epitaxy optimized for display applications and emitting in the visible blue range (wavelength  $\sim 450$  nm). This wafer was flipped and bonded, in a monolithic integration by non-aligned metal-metal bonding, to a Si(100) wafer that could be an ASIC in the final integration. The original Si(111) wafer is then removed via several steps of grinding and wet etching, and the GaN epitaxial wafer is etched using dry etching to create  $\mu\text{LED}$  pixels. Although such a process is more complex and requires more steps compared to the conventional process, it is compatible with ASIC thus better suited for industrial integration. Fig. 1a shows a cross-sectional diagram of the  $\mu\text{LED}$ s used in this work, and Fig. 1b shows a scanning electron microscopy (SEM) image of a  $\mu\text{LED}$ .

The commercial epitaxial stack used for these  $\mu\text{LED}$ s was grown in the conventional c-plane direction. C-plane GaN exhibits an internal electric field that spatially separates the wave functions of the electrons and holes [6]. This phenomenon, known as the Quantum-Confined Stark Effect (QCSE), leads to an increased recombination lifetime due to the reduced overlap between the two wave functions, thereby decreasing the modulation bandwidth. Consequently, for c-plane  $\mu\text{LED}$ s, a high current density ( $J$ ) of up to a few  $\text{kA}/\text{cm}^2$  is required to increase the modulation bandwidth to a few hundreds of MHz. Indeed, increasing  $J$  increases the carrier density in the  $\mu\text{LED}$ 's quantum wells, screening the internal field caused by QCSE and thus improving bandwidth [6]. The larger the  $\mu\text{LED}$ , the more current it requires to attain a sufficient bandwidth to reach Gb/s data rates, and thus the size of  $\mu\text{LED}$ s considered for this study ranged from  $10 \times 10 \mu\text{m}^2$  to  $50 \times 50 \mu\text{m}^2$ . Below this range, the optical power is insufficient, and above it, the required current, and thus voltage, is too high that it damages the isolation layers of the  $\mu\text{LED}$ .

## III. CHARACTERIZATION

### A. V-J-L Characteristics

Prior to data rate measurements, DC and RF characterizations of  $\mu\text{LED}$ s of different sizes were carried out using the experimental setup shown in Fig. 2a. Output optical power ( $L$ ) and current density ( $J$ ) versus input voltage ( $V$ ) of GaN-on-Si  $\mu\text{LED}$ s are shown on Fig. 3a. It can be seen from Fig. 3a that larger size GaN-on-Si  $\mu\text{LED}$ s show significantly larger output optical power due to their larger active area, where

for example, at  $J = 2 \text{ kA}/\text{cm}^2$ , the  $10 \times 10 \mu\text{m}^2$   $\mu\text{LED}$ 's optical power is  $14 \mu\text{W}$  compared to  $340 \mu\text{W}$  for the  $50 \times 50 \mu\text{m}^2$   $\mu\text{LED}$ .

### B. Modulation bandwidth

Bandwidth measurements were performed using a Rohde & Schwarz ZNL6 Vector Network Analyzer (VNA) with an RF signal input power of 0 dBm (1 mW). The bandwidth is evaluated as the 6-dB bandwidth of the forward transmission parameter ( $S_{21}$ ). The bandwidth was measured for  $\mu\text{LED}$ s of different sizes and at different current densities, as shown in Fig. 3b. As anticipated, bandwidth improves with increasing  $J$  by elevating the carrier density in the quantum wells, reducing QCSE. Regarding size dependency, Fig. 3b shows that the bandwidth is higher for larger  $\mu\text{LED}$ s. Modeling our  $\mu\text{LED}$ s based on [13] has shown that their RC time constant is around two orders of magnitude lower than the recombination lifetime. This means that the RC time constant has very limited influence on bandwidth, and thus the increase in bandwidth for larger-sized  $\mu\text{LED}$ s comes from a difference in recombination lifetime, which was also reported in [13]. This reduction in carrier lifetime with increasing size could be due to non-uniformity in carrier injection and is currently under investigation. Furthermore, we could evaluate the  $\mu\text{LED}$ s' impedance from the reflection S-parameter (i.e.  $S_{11}$ ) using the following equation:

$$Z_{LED} = Z_0 \times \frac{1+S_{11}}{1-S_{11}} \quad (1)$$

where  $Z_0$  is the characteristic impedance of the characterization circuit, which in our case is  $50 \Omega$ .

It was found that  $50 \times 50 \mu\text{m}^2$   $\mu\text{LED}$ s exhibit an impedance very close to  $Z_0 = 50 \Omega$  in the  $J$  range of 1 to  $2.3 \text{ kA}/\text{cm}^2$  (where  $S_{11} < -10$  dB), enhancing signal propagation to the  $\mu\text{LED}$ s, compared to smaller  $\mu\text{LED}$ s which require significantly higher  $J$  to achieve impedance matching.

From Fig. 3, it can be concluded that the use of larger  $\mu\text{LED}$ s will lead to a higher signal-to-noise ratio (SNR) at the receiver (due to the increased output optical power) and will offer a larger bandwidth. Consequently, we chose to use the  $50 \times 50 \mu\text{m}^2$   $\mu\text{LED}$  for conducting data rate measurements.

## IV. DATA COMMUNICATION USING GAN-ON-SI $\mu\text{LED}$ S

The experimental setup used to characterize the  $\mu\text{LED}$ s' data rate is shown in Fig. 4. The OFDM waveform is created using a Matlab<sup>®</sup> code, and then loaded onto an arbitrary waveform generator (AWG Tektronix AWG5202) to generate an analog OFDM signal. The output OFDM signal from the AWG then passes through two amplifiers (MiniCircuit ZFL-1000VH+) which amplifies the signal by 40 dB in total, before reaching a bias-tee (MiniCircuit ZFBT-4R2GW-FT), where it is coupled with a DC signal from a power supply (Keysight B2902A) to generate a DCO-OFDM modulation to turn on the  $\mu\text{LED}$  through a ground-signal-ground (GSG) RF probe (Titan T26A-GSG150). The output modulated light signal from the  $\mu\text{LED}$  is collected using a  $200 \mu\text{m}$  optical fiber (Thorlabs M136L02) that is connected to a high-speed photoreceiver (Femto HSPR-X-I-G4-SI) which integrates a trans-impedance amplifier (TIA) with a 1.4 GHz bandwidth to transform the optical signal into an electrical one. Then, the output electrical

signal is sent to a digital oscilloscope (Tektronix MSO64B) that is connected to a laptop, where the received digital signal is post-processed with Matlab. For OFDM generation, a Fast Fourier Transform (FFT) is used with  $N=1024$  points over a 5 GHz bandwidth, the inter-carrier spacing (ICS) is 4.88 MHz, the cyclic prefix size is only 8 samples since there is no significant delay spread to handle. OFDM signal is clipped at  $\pm 3.5\sigma$  to limit peak-to-average power ratio (PAPR) with respect to the  $\mu$ LED dynamic range, where  $\sigma$  is the standard deviation of the OFDM waveform. At transmission, we have finely tuned the modulation amplitude and bias voltage to ensure that we maximize optical modulation amplitude without significant impact from the  $\mu$ LED's non-linearity. At reception, post-processing on acquisitions consists of synchronization, demodulation and channel equalization. SNR at receiver is estimated using the transmission of known quadrature phase shift keying (QPSK) symbols, which are fed to a bit and power loading algorithm [4] that allocates quadrature amplitude modulation (QAM) constellation size and power to each OFDM subcarrier to optimize the data rate for a targeted Bit-Error-Rate (BER). Fig. 5a shows the evolution of received SNR and the number of allocated bits per OFDM subcarrier as a function of frequency for a 5.9 Gb/s DCO-OFDM transmission, achieved at a 7.8 V DC bias and a current of 59 mA (2.36 kA/cm<sup>2</sup>) with a modulation amplitude of 160 mV<sub>pp</sub> at the output of the AWG. Observing Fig. 5a reveals that the SNR dependency with frequency shows a higher 6-dB bandwidth compared to results shown in Fig. 3b. This can be attributed to the low-cut-off frequency (10 MHz) of the two identical amplifiers used in the transmitter for data rate measurements (but not used for  $\mu$ LED bandwidth measurements), which degrades the SNR of the lowest frequency OFDM subcarriers. Furthermore, a significant number of OFDM subcarriers is utilized beyond the 6-dB bandwidth of the  $\mu$ LED. This is expected because, in OFDM communication systems, data can be transmitted on subcarrier frequencies exceeding the bandwidth, provided there is sufficient SNR [14]. The additive white Gaussian noise (AWGN), primarily originating from receiver noise, imposes a major limitation for SNR, BER and consequently data rate. To address this limitation, signal averaging is performed on the received OFDM signal, serving as a method to evaluate the BER performance within a  $\mu$ LED distortion-limited scenario. As explained in [11], the averaging acquisition mode gives access to the  $\mu$ LED's performance when only its non-linear distortion noise is considered, discarding the impact of the receiver AWGN.

Fig. 5b shows the BER measurements as a function of the data rate for GaN-on-Si 50×50  $\mu$ m<sup>2</sup>  $\mu$ LED used in this work. The reference BER limit of  $3.8 \times 10^{-3}$  for efficient forward error correction (FEC) is reported on Fig. 5b as the dotted line. BER results on Fig. 5b (without averaging) show that 5.9 Gb/s data rate can be obtained with GaN-on-Si  $\mu$ LEDs which is slightly lower than with conventional GaN  $\mu$ LED grown on Sapphire. However, a data rate of 15.5 Gb/s was obtained when using the averaging mode of the oscilloscope (taking multiple acquisitions and averaging them together). This result indicates that  $\mu$ LEDs used in this work achieve better linearity compared to those used in [11], showing high potential data rates if a dedicated receiver is employed.

Fig. 6 shows a comparison of this work with results from the literature, with both single- $\mu$ LED measurements and series-arrays of  $\mu$ LEDs. In works [2] and [10], where series-array of  $\mu$ LEDs are used, we considered the area as that of one  $\mu$ LED multiplied by their number. On Fig. 6, the largest data rates are obtained with optical OFDM modulation technique, exhibiting superior spectral efficiency as compared with non-return to zero on-off keying (NRZ-OOK). The GaN-on-Si  $\mu$ LED used in this work achieves a lower data rate (without signal averaging) than the best GaN  $\mu$ LEDs grown on free-standing GaN or Sapphire, while the distortion-limited performance of GaN-on-Si  $\mu$ LED (with signal averaging) exhibits a significantly high data rate compared to the literature. Note that such distortion-limited performance of  $\mu$ LEDs could be approached by reducing AWGN noise (i.e. reducing detected receiver noise) by using dedicated reception circuits instead of a commercial off-the-shelf (COTS) photodiode as done in this work.

## V. CONCLUSION

In this paper, we have reported data rate measurements using a blue (In)GaN  $\mu$ LED reported on a Silicon wafer compatible with ASIC processes for complete transceiver integration, dedicated for the next generation of  $\mu$ LED arrays for parallel interconnects and optical wireless communication systems. By applying DCO-OFDM modulation technique with a bit loading algorithm on a 50×50  $\mu$ m<sup>2</sup> GaN-on-Si  $\mu$ LED, a data rate of 5.9 Gb/s is measured for a BER corresponding to the FEC limit. Although the optical power and bandwidth of  $\mu$ LEDs used in this work are lower than those of state-of-the-art GaN  $\mu$ LEDs, they were able to reach comparable data rates thanks to their high linearity. Achieving such a data rate on  $\mu$ LEDs grown on 200-mm Silicon wafers, compared to the smaller and more expensive GaN or Sapphire substrates usually used for GaN  $\mu$ LEDs, marks a significant step towards large-scale industrial integration. Moreover, the distortion-limited achievable data rate of this GaN-on-Si  $\mu$ LED is evaluated at 15.5 Gb/s by averaging several acquisitions to reduce AWGN, demonstrating promising obtainable results using a dedicated reception circuit in future integrations. Since carrier lifetime has been identified as the main factor for bandwidth limitation, future enhancements in the  $\mu$ LEDs' epitaxial structure will aim to reduce it. Improving epitaxial quality will also be targeted to reduce defects and thus improve quantum efficiency to increase optical power. Enhancements of the electrical contact will also be investigated to reduce resistance, thereby limiting the required driving voltage, decreasing power consumption.

## REFERENCES

- [1] F. Templier *et al.*, "High-resolution active-matrix 10- $\mu$ m pixel-pitch GaN LED microdisplays for augmented reality applications", Proc. SPIE 10556, *Advances in Display Technologies VIII*, 105560I, 2018; <https://doi.org/10.1117/12.2294527>.
- [2] E. Xie *et al.*, "Over 10 Gbps VLC for Long-Distance Applications Using a GaN-Based Series-Biased Micro-LED Array," *IEEE Photonics Technol. Lett.*, vol. 32, no. 9, pp. 499–502, 2020, doi: 10.1109/LPT.2020.2981827.
- [3] Z. Wei *et al.*, "Multigigabit Visible Light Communication Based on High-Bandwidth InGaN Quantum Dot Green Micro-LED," *ACS Photonics*, vol. 9, no. 7, pp. 2354–2366, 2022, doi: 10.1021/acsp Photonics.2c00380.
- [4] L. Maret, L. N. Dinh, A. Lagrange, P. Demars, L. Dupr, and O. Lartigue, "Reaching 7.7 Gb / s in VLC with DCO-OFDM on a single GaN Blue Micro-LED," *Opt. Wirel. Commun. Conf.*, vol. 2, pp. 1–4, 2020.

- [5] B. Pezeshki, F. Khoeini, A. Tselikov, R. Kalman, C. Danesh, and E. Afifi, "MicroLED Array-based Optical Links Using Imaging Fiber for Chip-to-chip Communications," *Opt. InfoBase Conf. Pap.*, pp. 1–3, 2022, doi: 10.1364/ofc.2022.w1e.1.
- [6] A. Rashidi, M. Monavarian, A. Aragon, A. Rishinaramangalam, and D. Feezell, "Nonpolar m-Plane InGaN/GaN Micro-Scale Light-Emitting Diode with 1.5 GHz Modulation Bandwidth," *IEEE Electron Device Lett.*, vol. 39, no. 4, pp. 520–523, Apr. 2018, doi: 10.1109/LED.2018.2803082.
- [7] J. Vinogradov *et al.*, "GaN-based cyan light-emitting diode with up to 1-GHz bandwidth for high-speed transmission over SI-POF," *IEEE Photonics J.*, vol. 9, no. 3, pp. 1–7, 2017, doi: 10.1109/JPHOT.2017.2693207.
- [8] M. Akhter *et al.*, "200 Mbit/s data transmission through 100 m of plastic optical fibre with nitride LEDs," *Electron. Lett.*, vol. 38, no. 23, pp. 1457–1458, 2002, doi: 10.1049/el:20021004.
- [9] F. Rao *et al.*, "10.5 Gbps visible light communication systems based on c-plane freestanding GaN micro-LED," *J. Light. Technol.*, pp. 1–6, 2024, doi: 10.1109/jlt.2024.3363729.
- [10] R. Lin *et al.*, "High bandwidth series-biased green micro-LED array toward 6 Gbps visible light communication," *Opt. Lett.*, vol. 47, no. 13, p. 3343, 2022, doi: 10.1364/ol.1458495.
- [11] M. S. Islim *et al.*, "Towards 10 Gb/s orthogonal frequency division multiplexing-based visible light communication using a GaN violet micro-LED," *Photonics Res.*, vol. 5, no. 2, p. A35, 2017, doi: 10.1364/prj.5.000a35.
- [12] S. J. Kim, S. Oh, K. J. Lee, S. Kim, and K. K. Kim, "Improved performance of GaN-based light-emitting diodes grown on si (111) substrates with nh3 growth interruption," *Micromachines*, vol. 12, no. 4, pp. 1–8, 2021, doi: 10.3390/mi12040399.
- [13] A. Rashidi *et al.*, "Differential carrier lifetime and transport effects in electrically injected III-nitride light-emitting diodes," *J. Appl. Phys.*, vol. 122, no. 3, 2017, doi: 10.1063/1.4994648.
- [14] S. Mardankorani, X. Deng and J. -P. M. G. Linnartz, "Optimization and Comparison of M-PAM and Optical OFDM Modulation for Optical Wireless Communication," in *IEEE Open Journal of the Communications Society*, vol. 1, pp. 1721-1737, 2020, doi: 10.1109/OJCOMS.2020.3034204.

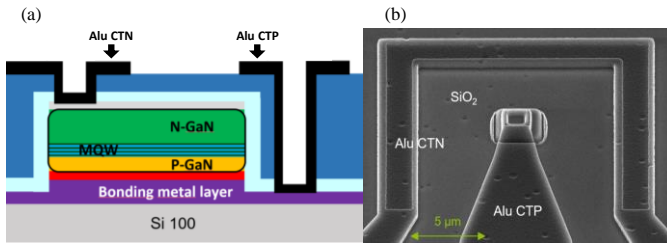


**Fig. 1.** a.  $\mu$ LED cross view. The P-GaN is on the wafer side, meaning that the PN junction is flipped compared to conventional structures. b. SEM photo of a  $\mu$ LED.

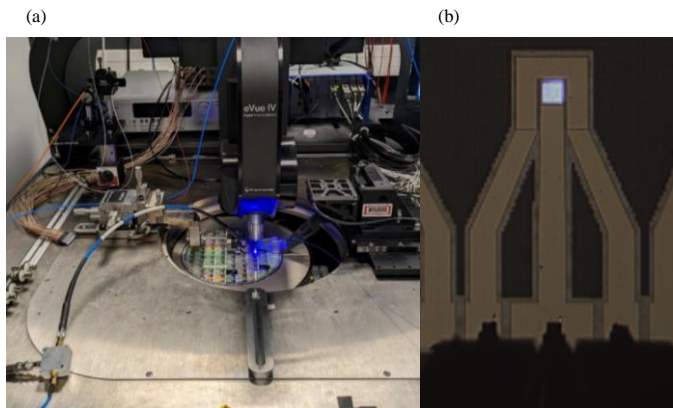


**Fig. 2.** a. Picture of our experimental setup with the  $\mu$ LED lighted on, b. Picture from the microscope showing the lighted on  $50 \times 50 \mu\text{m}^2$   $\mu$ LED with the probe in contact.

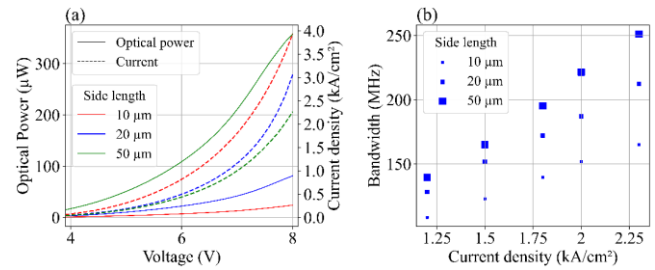


**Fig. 3.** a. Optical power and current density versus voltage and b. modulation bandwidth of  $\mu$ LEDs versus current density for  $\mu$ LEDs of difference sizes.

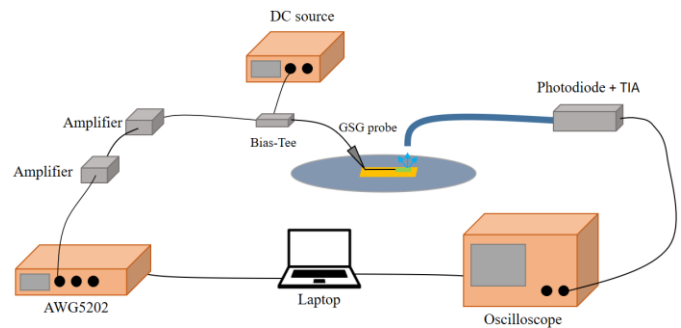


**Fig. 4.** Schematic of the experimental setup used to perform the DCO-OFDM data rate measurements.

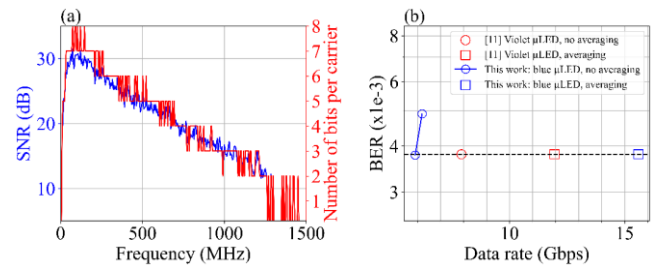


**Fig. 5.** a. SNR and carrier loading of the 5.9 Gb/s transmission. b. Data rate versus BER of our  $\mu$ LEDs with and without averaging compared to results from the literature with and without averaging.

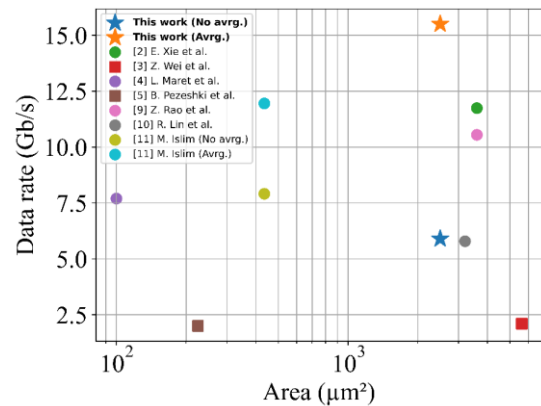


**Fig. 6.** Comparison of data rates versus active area of GaN  $\mu$ LEDs. Square markers refer to NRZ-OOK modulation, while the circular ones represent OFDM.